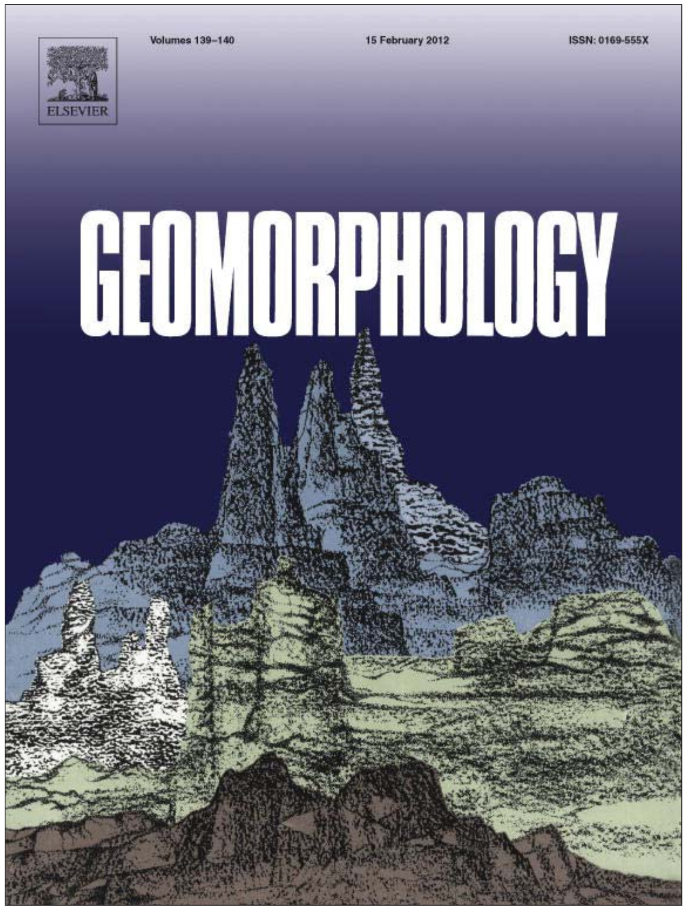
Volumes 139–140
15 February 2012
ISSN: 0169-555X
ELSEVIER
GEOMORPHOLOGY

Geomorphology 139–140 (2012) 425–437

Contents lists available at SciVerse ScienceDirect

Geomorphology

journal homepage: www.elsevier.com/locate/geomorph

Event-based suspended sediment dynamics in a central New York watershed

Peng Gao *, Maria Josefson

Department of Geography, Syracuse University, Syracuse, NY 13244, USA

ARTICLE INFO

Article history:
Received 29 June 2011
Received in revised form 8 November 2011
Accepted 9 November 2011
Available online 15 November 2011

Keywords:
Sediment dynamics
Suspended sediment transport
Hysteresis pattern
Hysteresis analysis
Event sediment yield

ABSTRACT

Using discharge and sediment data collected from 23 events between 2008 and 2010 in a 311-km^2 watershed of central New York, we investigated event sediment dynamics of the studied watershed. After showing the statistical difference of the data in different seasons, we examined the detailed hysteresis patterns of all events. Spring events had figure eight with anticlockwise (figure-8/AC), clockwise (C), anticlockwise (AC), and complicated patterns. Summer events had C, AC, figure-8/AC, figure-8/C, and complicated patterns. Fall and winter events had the same patterns as those in summer, as well as a weak loop pattern. The diversity of patterns within and between seasons suggests that detailed processes of sediment transport were not only complicated during one event but also varied from season to season. Although hysteresis analysis failed to identify these detailed processes and the associated sediment sources in such a relatively large watershed, it successfully revealed a common feature dominating the transport processes: event sediment transport was generally supply limited. Further analysis on the correlation between event sediment yield (SSY_e) and event peak discharge (Q_{peak}) indicated that (i) events with clockwise patterns tended to have more SSY_e than those with other patterns for the same Q_{peak} and (ii) data from all events may be statistically well described by a single SSY_e–Q_{peak} equation, regardless of hysteresis patterns. This equation (i) reveals that complicated event transport processes may be lumped into a simple process over events and (ii) reflects the general supply-limited nature identified by hysteresis analysis. Using this equation and the magnitude–frequency analysis, we further discovered that in the past 21 years, sediment was mainly transported by more frequent but relatively small discharges with the recurrence interval no more than 0.5 year.

1. Introduction

Event sediment dynamics refer to various processes involved in suspended sediment transport through a watershed during a hydrological event. A fundamental feature of suspended sediment transport during an event is that suspended sediment concentration (*SSC*) is often not in phase with the associated water discharge (*Q*), such that a single sediment rating curve (SRC) is often hard to describe the *SSC*–*Q* relationship for one event, one season, or one year (Walling, 1977; Walling and Webb, 1982). This feature has been commonly studied using a technique called hysteresis analysis, in which physical processes of sediment transport are qualitatively identified in terms of the direction of a hysteresis loop (de Boer and Campbell, 1989; Williams, 1989). According to a systematic classification, hysteresis loops may have five basic patterns (Williams, 1989), three of which (i.e., clockwise, anticlockwise, and figure eight) have been commonly observed in various watersheds (Klein, 1984; Park, 1992; Asselman, 1999; Brasington and Richards, 2000; Richards and Moore, 2003; Seeger et al., 2004), though more complicated ones have also been reported (de Boer and Campbell, 1989; Gao and Pasternack, 2007; Smith and Dragovich, 2009). A clockwise loop usually means that sediment is primarily originated from stream channels causing the first-flush effect, supplied from upstream hillslopes leading to the sediment depletion effect, or due to the successive reduction of the erosive effect of rainfall (Jansson, 2002; Wotling and Bouvier, 2002; Rovira and Batalla, 2006; Gao and Pasternack, 2007). An anticlockwise loop tends to reflect sufficient hillslope sediment supply, delayed in-channel sediment resuspension caused by the late break-up of biofilms, additional sediment sources from channel banks or tributaries, or variable rainfall patterns (Lawler et al., 2006; Gao, 2008; Lopez-Tarazon et al., 2009; Mano et al., 2009). A figure-eight loop could be the result of transporting suspended sediment of heterogeneous sizes (Smith and Dragovich, 2009) or a combination of multiple processes (Seeger et al., 2004).

These patterns were identified based on a single-peak hydrograph (Williams, 1989). In reality, however, hydrographs with multiple peaks are not uncommon if rainfall is prolonged or variable (Seeger et al., 2004; Sadeghi et al., 2008a). Such hydrographs can easily produce more complicated hysteresis loops in addition to the three patterns described above (Rieger et al., 1988; Lecce et al., 2006) indicating more complicated transport processes in these events. Hence, the connection between event sediment dynamics and the resultant hysteresis patterns is highly variable. In watersheds with relatively small areas (e.g., area < 10 km^2), hysteresis loops have been

* Corresponding author. Tel.: +1 315 443 3679.
E-mail address: pegao@maxwell.syr.edu (P. Gao).

0169-555X/$ – see front matter © 2011 Elsevier B.V. All rights reserved.
doi:10.1016/j.geomorph.2011.11.007

linked to specific factors such as soil moisture conditions, the difference between throughflow and storm flow, or gullied channel bank erosion (Seeger et al., 2004; Langlois et al., 2005; Lefrancois et al., 2007; Sadeghi et al., 2008b; Smith and Dragovich, 2009). As the watershed area increases, more physical processes (e.g., overland and subsurface flows) and environmental conditions (e.g., soil types, land use and land cover patterns, topography) are involved in event sediment transport. Consequently, a hysteresis pattern is often the result of multiple processes and thus is hard to be linked to a single factor. This may explain why hysteresis analysis has not been used to systematically identify event-based sediment dynamics in watersheds with relatively large areas (e.g., $A > 100\ \text{km}^2$), though description of hysteresis loops in large watersheds may be found sporadically (Picouet et al., 2001; Oeurng et al., 2010).

However, to what extent hysteresis analysis can reveal event sediment dynamics of relatively large watersheds is still not clear. We thus studied event sediment dynamics of a medium-sized (based on the classification of Singh, 1995) watershed in central New York using hysteresis analysis. The study was based on the collected discharge and sediment data from hydrological events between 2008 and 2010. In particular, we first described the statistical characteristics of four event variables relevant to water discharges and sediment concentrations and their seasonal variations. Then we analyzed hysteresis patterns of events in each season. Subsequently, we examined the relationship between event sediment yields and event peak discharges. Finally, we discussed the averaged long-term trend of sediment dynamics in the studied watershed using the frequency–magnitude analysis.

2. Study site and methods

2.1. Study site

The studied watershed occupies the upper and middle portions of Oneida Creek watershed with an area of 311 km^2. Its elevation ranges from 570 m at the southwestern end to 120 m at the outlet, with greater slope variations in the upstream region and relatively gentle slopes in the downstream area. The typical dendritic stream network consists of the main stream, Oneida Creek (the fourth-order stream) and the main tributary, Sconondoa Creek (the third-order stream), together draining into Oneida Lake (Fig. 1). The studied watershed has the drainage density of 1.3, suggesting that it is a highly divided

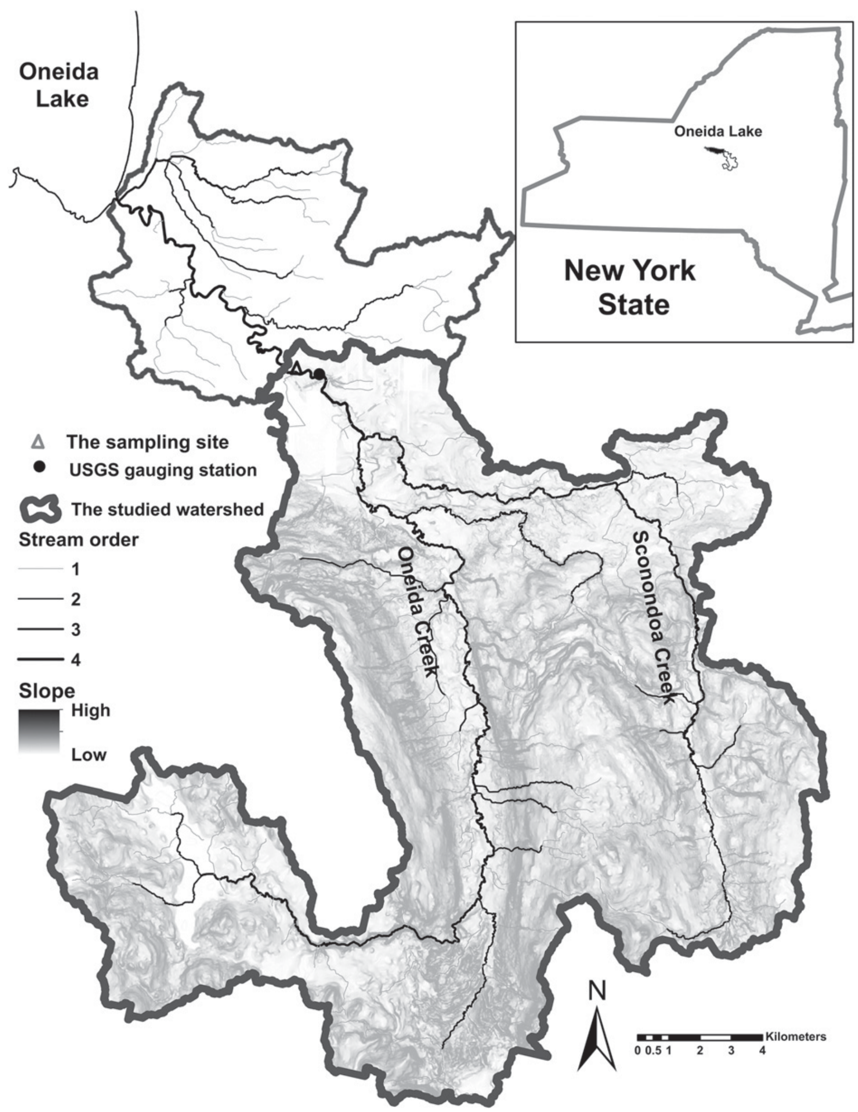

Fig. 1. The studied watershed in central New York.

drainage basin with a relatively rapid response to rainfall events (Yildiz, 2004).

The watershed's humid continental climate brings in about 1270 mm precipitation annually and shows significant seasonal variations. Summer is warm with moderate rainfall. The prolonged winter is cold and snowy (snow is mainly supplied by lake-effect snow). Fall is relatively wet, and spring is characterized by the mixture of snowmelt and rainfall. Land use and land cover (LULC) in the studied watershed is composed of 50% agricultural lands, 23% forest, 13% grass lands, 7% urban lands, and 5% others (e.g., wetlands). Approximately 67% of the soils in the watershed are constrained for agricultural use because of high erosion rates (Domack et al., 2004). The LULC is also subject to seasonal changes: more ground cover in fall owing to falling leaves and mature vegetation, relatively less ground cover in winter and spring.

2.2. Methods

2.2.1. Event data collection

We installed an ISCO automatic pumping sampler at the outlet of the studied watershed to collect event-based samples from 2008 to 2010 (Fig. 1). A threshold value that triggers sampling was set before each event based on latest base-flow level and weather forecast of the coming event. Sampling intervals were set between 1 and 4 h depending on the predicted event duration and magnitude. Selection of the threshold value and sampling interval was essentially a trial-and-error process, which resulted in missing some fall events that we planned to capture. The collected samples were analyzed using the standard gravimetric method to obtain suspended sediment concentration (*SSC*). Water levels of the sampled events were correlated to those at a nearby USGS gauging station, which is located about 1.0 km upstream of the sampling site (Fig. 1). This relationship, together with the established stage–discharge relationship at the USGS gauging station, was subsequently used to calculate water discharges (Q) of monitored events at the sampling site. No event was purposely selected for sampling. Throughout the three-year study period, we tried to sample as many events as we practically could. Thus, sampling was not biased for any given subset of all events.

The collected samples were point samples, which may not necessarily be representative of the mean along the cross section (Hicks and Gomez, 2003). For a low flow rate, we collected three depth-integrated samples using a USGS DH-48 suspended sampler at three different locations along the cross section and compared their *SSC* values to that of the sample collected at the regular location by the ISCO sampler around the same time. The difference was negligible. We cannot sample in stream during high flows when the stream is not wadeable. However, particle size analysis for samples from several events showed that suspended sediment is predominantly made up of silt and clay with the median size D_{50} ranging from 0.04 to 1.3 mm, which are much less than $D_{50}=10$ mm of bed materials at the sampling site. So, we assume that suspended sediment in most of the events was well mixed and *SSC* values of the collected point samples are approximately equivalent to their cross section means.

2.2.2. Statistic and hysteresis analyses

For each event, both mean and peak water discharges and *SSCs* (i.e., Q_{mean}, Q_{peak}, SSC_{mean} and SSC_{peak}) were calculated. The associated event sediment yield (SSY_e) was determined using the method described below. Descriptive statistics and a two-sample different test were performed for these four variables of events in different seasons to identify seasonal patterns of both Q and *SSC*. In each season, hysteresis patterns of sampled events were generated and analyzed. These patterns were linked to the possible sediment sources and dominant transport processes of the events. Although the magnitude and direction of a hysteresis loop have been quantified by a single index H (Langlois et al., 2005), which is defined as the ratio of the total sediment load of the rising limb to that of the falling limb, this index failed to characterize the hysteresis nature of an event. For example, if an event has no hysteresis effect, but a left-skewed hydrograph, the theoretical value of the index H should be one, whereas the calculated H by definition will be less than one. A different index HI was also developed based on the shape of a hysteresis loop (Lawler et al., 2006). Calculating HI involves two steps. First, determine mid-point discharge Q_{mid} by $Q_{mid}=k\ (Q_{max}-Q_{min})+Q_{min}$ where $k=0.5$ for Q_{mid} and Q_{min} and Q_{max} are minimum and maximum discharges, respectively. Second, interpolate *SSC* values on both limbs for the same Q_{mid} (C_{rise} and C_{fall}) and calculate HI for a clockwise loop by $HI=(C_{rise}/C_{fall})-1$ and for an anticlockwise loop by $HI=(-1/(C_{rise}/C_{fall}))+1$. Because Q_{mid} can only be clearly identified for simple patterns such as clockwise and anticlockwise loops, significant uncertainties are involved when HI is calculated for more complicated patterns. Therefore, neither H nor HI may provide more reliable information than the classic visual analysis does. For this reason, we adopted the latter in hysteresis analysis.

2.2.3. Examination of the relationship between SSY_e and Q_{peak}

A critical step of determining SSY_e is to establish sediment rating curves (SRCs) for the selected events. Because the hysteresis effect appeared in most of the selected events, using a single SRC for an

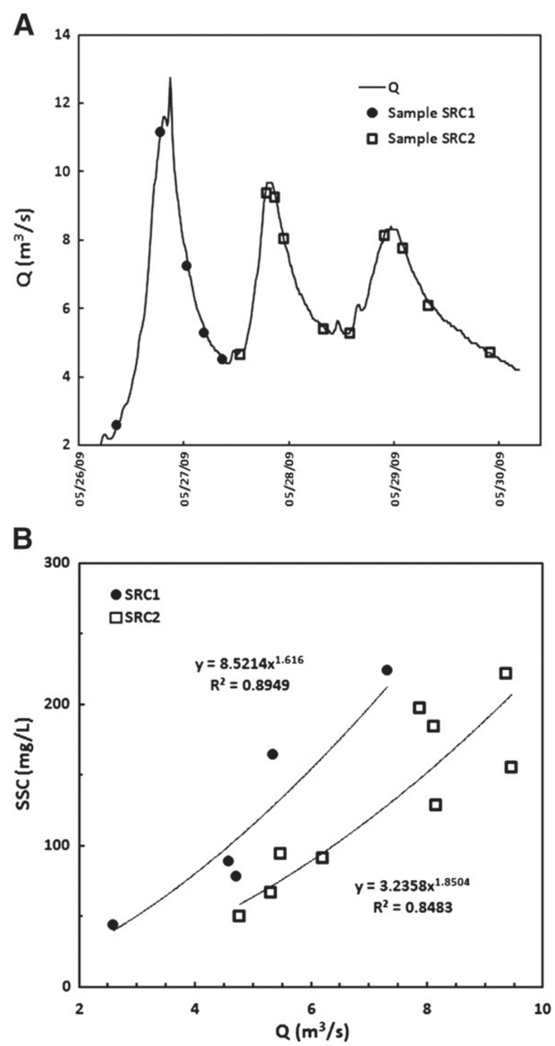

Fig. 2. Sediment rating curves (SRCs) for the 5/27/2009 event. (A) Sediment samples with respect to the hydrograph; (B) two different SRCs.

Table 1
Statistical properties of all selected events.

Season	Events	Patterns	Q_{mean} m^3/s	SSC_{mean} mg/l	Q_{peak} m^3/s	SSC_{peak} mg/l	SSY_e t
Spring	4/3/2009	Figure-8/AC	18.18	112.10	32.49	444.97	1106.55
Spring	4/21/2009	C	4.78	164.23	6.09	426.02	125.79
Spring	5/16/2009	Complicated	4.38	80.80	6.01	137.02	42.92
Spring	5/27/2009	Complicated	6.68	137.92	12.74	520.44	294.14
Spring	6/11/2009	Figure-8/AC	3.62	52.51	6.01	116.80	29.44
Spring	6/5/2010	AC	6.74	318.45	19.17	1014.79	513.33
Mean			7.40	144.34	13.75	443.34	352.03
CV			0.73	0.65	0.77	0.74	1.17
Summer	7/13/2008	Figure-8/AC	6.36	183.3	9.81	410.4	102.85
Summer	7/27/2008	AC	6.30	1099.35	11.96	2208.77	885.96
Summer	8/11/2008	C	14.40	1443.95	30.30	9441.06	2764.70
Summer	7/31/2009	Complicated	3.05	84.76	6.49	246.74	108.06
Summer	6/23/2010	AC	8.67	293.19	24.26	1273.00	605.81
Summer	6/28/2010	Figure-8/AC	11.92	388.67	37.10	2165.69	2042.34
Summer	7/23/2010	Complicated	7.41	130.32	16.67	273.75	297.54
Summer	8/22/2010	Figure-8/C	16.94	215.58	64.08	1152.81	2900.16
Mean			9.38	479.89	25.08	2146.53	1213.43
CV			0.50	1.05	0.76	1.42	0.97
Fall	9/30/2010	Figure-8/C	32.44	370.22	88.26	1433.15	5845.72
Fall	11/20/2009	Figure-8/AC	5.89	172.13	9.97	538.05	164.00
Fall	12/1/2010	Complicated	31.34	682.70	70.49	1877.99	5579.60
Winter	12/27/2009	AC	8.29	179.65	13.22	358.19	387.82
Winter[a]	1/25/2010	C	35.08	1236.74	97.71	3400.48	15958.79
Winter[a1]	3/11/2010	Weak loop	24.73	1123.10	33.21	1730.88	2505.38
Winter[a2]	3/12/2010	C	26.95	2497.42	33.21	2497.43	7113.65
Winter[a3]	3/13/2010	C	22.84	1716.38	23.98	2101.39	2410.27
Winter[a6]	3/16/2010	AC	20.93	1193.87	23.42	1396.61	2226.45
Mean			23.14	1324.53	37.46	1914.16	5100.39
CV[b]			0.38	0.58	0.81	0.54	1.13

[a] This is a snowmelt dominated event with some rainfall, [a1] to [a3] and [a6] are the four selected events in a series of snowmelt events.
[b] CV refers to coefficient of variance.

entire event may cause a relatively large error in estimating SSY_e for some events. To avoid this, we first inspected the patterns of the sampled data for each event. If the data demonstrated multiple patterns, then we developed separate SRCs for different patterns. For example, in the 5/27/2009 (May 27, 2009) event (Fig. 2A), the sediment data showed two different trends over the event (Fig. 2B). We then developed two different SRCs for the two trends (Fig. 2B). When calculating SSY_e, we applied each SRC to the associated discharge range to calculate suspended sediment transport rate (Q_s, kg/s) at each discharge interval within the range. Then, we calculated SSY_e by summing $Q_{si}t_i$ over the whole range of the hydrograph, where $t_i = 15$ min is the time interval between two consecutive discharges. We should note that data trends were often not in phase with limbs — that is, one trend could cover the rising limb and a part of the falling limb, while the other may just cover the remaining part of the falling limb. Therefore, developing SRCs based on the data trends can produce more accurate estimation of SSY_e than simply developing SRCs in terms of the limbs. Because previous studies showed that SSY_e tends to be related to peak discharges (Q_{peak}) (Hicks, 1994; Schmidt and Morche, 2006), values of SSY_e were subsequently correlated with Q_{peak} for events of different seasons and all events, respectively.

3. Results and analysis

3.1. Selected events and their statistical characteristics

Forty-six (46) events were sampled throughout all four seasons from 2008 to 2010 (7 in 2008, 19 in 2009, and 20 in 2010). Scrutiny of these data revealed that (i) data in some events only spanned either the rising or falling limb and (ii) only a few (less than four) data points were sampled in some events. For these events, we are not sure whether sediment data can reflect sediment dynamics of the whole event and thus how much errors might be involved in the subsequent hysteresis analysis and event load estimation. Eliminating these events led to 23 events, with six in spring, eight in summer, three in fall, and six in winter (Table 1). Comparing values of Q_{peak} in the finally selected events in each season with those of all events of the same season in the study period indicated that these Q_{peak} values almost spanned the full range of all Q_{peak} values in each season. For example, Q_{peak} values of all spring events from 2008 to 2010 ranged from 2.51 to 51.62 m^3/s and for all fall events changed from 5.12 to 88.26 m^3/s. These two ranges are similar to those of the selected events in these two seasons (Table 1). The similarity suggests that though the number of finally selected events is considerably reduced, these events are still representative of the variation of events in each season.

Values of Q_{mean}, Q_{peak}, SSC_{mean}, and SSC_{peak} in fall had similar ranges to those in winter (Table 1), suggesting that fall apparently showed similar characteristics of sediment transport to winter, though the small number of events in fall makes any statistical analysis inappropriate. The descriptive statistics for the remaining three seasons showed that spring had the lowest values of average Q_{mean}, Q_{peak} (7.4 and 13.75 m^3/s), SSC_{mean}, SSC_{peak} (144.34 and 443.34 mg/l), and SSY_e (352.03 t); while winter had the highest values (23.14 and 37.46 m^3/s, 1324.53 and 1914.16 mg/l, and 5100.39 t) (Table 1). However, sediment loads in these seasons showed similar degree of variations (i.e., similar values of coefficient of variance, CV).

A two-sample difference test revealed that values of Q_{mean} and SSC_{mean} in spring and summer were not statistically different from each other but were statistically different from those in winter. However, the two peak variables (Q_{peak} and SSC_{peak}) had a different seasonal pattern. While their values in spring and winter were statistically different, their summer values were statistically similar to those in spring and winter, respectively. Descriptive statistics and statistic tests demonstrated that discharges and sediment concentrations (and thus sediment loads) were generally high in winter and low in spring.

3.2. Hysteresis patterns of events

3.2.1. Spring

In spring, six events displayed four different hysteresis patterns: figure eight with anticlockwise (figure-8/AC), clockwise (C), anticlockwise (AC), and complicated loops (Table 1). In the figure-8/AC pattern of the 4/3/2009 event (Fig. 3A), an anticlockwise loop in the middle indicated that *SSC* during the rising stage was lower than that during the falling stage. This loop most possibly suggests that suspended sediment carried from far uplands needed a longer time to arrive at the outlet. The reasons are (i) the studied watershed has a relatively large area ($A = 311\ km^2$) and (ii) upstream branches have significantly steeper channel slopes, such that sediment brought from their contributing areas during the precedent event was hardly deposited to serve as in-channel sediment sources for the current event. The end of the falling limb was lower than the beginning of the rising limb, suggesting the depletion effect — that is, suspended sediment supplied from upland sources was limited. The clockwise loop during the 4/21/2009 event (Fig. 3B) suggested that sediment was primarily from near stream channels with limited upland sediment displacement causing the relatively low SSC values (though they increased with the decrease of Q) toward the end of the falling limb. The complicated pattern of the 5/16/2009 event had a sharp sediment increase at the beginning of the rising limb that was caused by a discharge pulse (Fig. 3C). Because the local Q_{peak} arrived earlier than local C_{peak}, sediment should be displaced from near-channel areas. The following anticlockwise loop clearly suggested that subsequent sediment was from upland sources and traveled a relatively long distance owing to the large size of the studied watershed. The consistent sediment decrease close to the end of the falling limb signified the depletion effect. In the only anticlockwise pattern of the 6/5/2010 event (Fig. 3D), the rapid increase of Q during the rising limb resulted in the C_{peak} arrival later than Q_{peak}, suggesting that sediment was mainly from upland sources. Furthermore, the continuous and prompt decrease of *SSC* during the falling limb inferred that sediment supply from upland sources was inadequate. The interpretation of the anticlockwise pattern is contrary to that for the same pattern in a small watershed where higher *SSCs* in the falling limb indicated sufficient sediment supply from the upland sources (Lawler et al., 2006). If sediment supply in the studied watershed were ample in this event, the slope of the falling limb would become gentle toward the end. This difference highlights the area effect on the interpretation of a hysteresis pattern.

The complexity of event-based sediment dynamics in spring was reflected by not only the diversity of hysteresis patterns but also the inconsistency between these patterns and the associated discharges. For example, events with different amounts of discharges could result in the same hysteresis pattern (i.e., the figure-8/AC patterns for 4/3/2009 and 6/11/2009), whereas events with similar discharges could lead to different hysteresis patterns (i.e., C in 4/21/2009, but

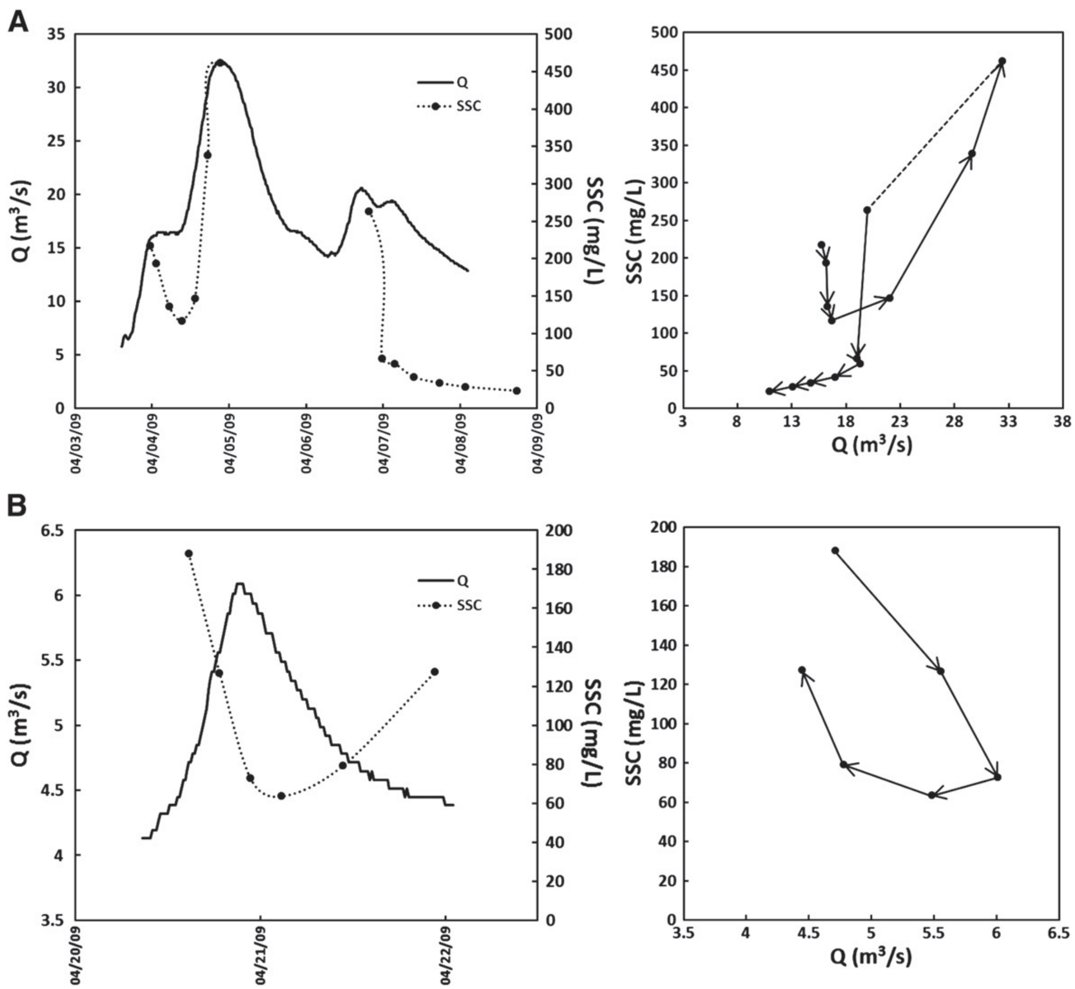

Fig. 3. Different types of hysteresis patterns in spring. (A) A figure-8/AC loop in the 4/3/2009 event, (B) a clockwise loop in the 4/21/2009 event, (C) a complicated loop in the 5/16/2009 event, and (D) an anticlockwise loop in the 6/5/2010 event.

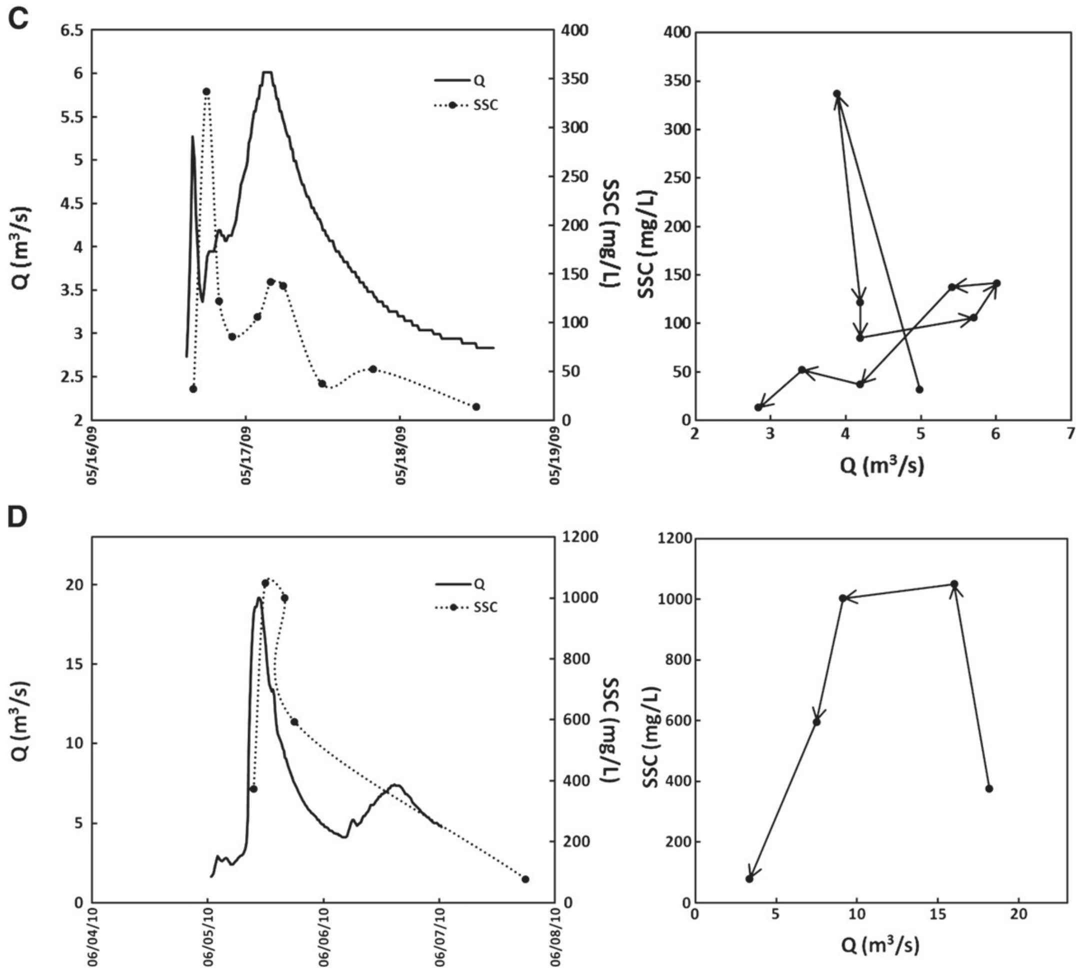

Fig. 3 (*continued*).

complicated in 5/16/2009) (Table 1). Nonetheless, all events, regardless of specific hysteresis patterns, showed a common property: sediment transport experienced the depletion effect over events. This suggests that, in spring, suspended sediment transport in the studied watershed was primarily controlled by the supply-limited process.

3.2.2. Summer

Rainfall events in summer produced five hysteresis patterns: C, AC, figure-8/AC, figure-8/C, and complicated loops (Table 1). Similar to those in spring, the two complicated patterns were caused by multiple discharge peaks of the events. The first two discharge peaks in the event of 7/31/2009 gave rise to a clockwise subloop showing the depletion effect toward the end of the second falling limb (Fig. 4A), whereas the last two peaks generated a figure-8/AC subloop, suggesting the limited sediment supply from upland sources because *SSC* values at the end of the last falling limb were low. The other event with a complicated pattern (i.e., 7/23/2010) demonstrated a similar supply-limited transport process, though it occurred in a different year with much larger discharges (Table 1). Despite their significantly different Q_{peak} values, the two events (i.e., 7/13/2008 and 6/28/2010) generated the same figure-8/AC pattern with significantly low *SSC* values toward the end of the falling limb, suggesting the prevalence of the supply-limited nature of sediment transport. The figure-8/C pattern in the 8/22/2010 event (Fig. 4B) demonstrated an earlier arrival of C_{peak} during the rising limb, suggesting the in-channel sediment supply. The *SSC* values decreased promptly along the falling limb, signifying the limited sediment supply from upland sources. In the event of 8/11/2008, the clockwise loop (Fig. 4C) indicated that C_{peak} arrived earlier than Q_{peak}, suggesting the dominance of in-channel sediment sources. The consistent decrease of *SCC* values in the falling limb suggested the limited upland sediment supply, which was interrupted by a sudden *SSC* increase toward the end, suggesting the existence of a local sediment source near the sampling site. In the remaining two events that had the same anticlockwise pattern, the earlier arrived Q_{peak} than C_{peak} showed that sediment was mainly supplied from upland sources. Yet, the lower *SSC* values toward the end of the falling limb than those toward the beginning of the rising limb (see Fig. 4D for the 7/27/2008 event) suggested that the supply-limited process dominated sediment transport in these two events.

Variable hysteresis patterns of summer events again showed that detailed sediment dynamics within each event may be quite different. However, event sediment transport was generally controlled by the supply-limited nature.

3.2.3. Fall and winter

Fall events involved a figure-8/C, figure-8/AC, and complicated patterns; while winter events included an AC and C patterns, as well as a series of snowmelt events (Table 1). The figure-8/C pattern of the 9/30/2010 event (Fig. 5A) indicated that suspended sediment was mainly supplied from stream channels (Table 1). This was evidenced by its Q_{peak} value, which was the highest among those of rainfall-induced events and caused a series of bank erosion in Oneida Creek that was observed after the event. The significant and sharp decrease of *SSC* values toward the end of the falling limb suggested that sediment supplied from upland sources was limited. The figure-8/AC pattern in the 11/20/2009 event showed a similar style to the 6/11/2009 event in spring with comparable Q_{peak}, during which sediment transport was controlled by the supply-limited process. In the 12/1/2010 event with a complicated pattern, the abrupt increase of discharge during the rising limb was associated with timely increased sediment concentration (Fig. 5B), suggesting that sediment was mainly supplied from stream channels. During the falling limb, the constant *SSC* decrease revealed that sediment supply from upland sources was limited. The AC pattern of the winter rainfall event (i.e., 12/27/2009) suggested that limited sediment was supplied from upland sources because *SSC* values toward the end of the falling limb were lower than those around the beginning of the rising limb (Fig. 5C). These rainfall-induced events displayed a similar supply-limited process dominating event-based sediment transport to that in spring and summer.

The snowmelt event (1/25/2010) was characterized by a clockwise loop suggesting that sediment was mainly from in-stream channels. This is consistent with the fact that uplands were covered by snow and hardly produced significant sediment. The last four winter events (Table 1) belonged to a series of snowmelt events (Fig. 5D), three out of which (events 1, 3, and 6) experienced significant decrease of sediment concentrations during the falling limbs. This concentration decrease highlighted the supply-limited nature of sediment transport in these events, irrespective of their hysteresis patterns. The remaining event (event 2) showed an increase of sediment toward the end of the falling limb (Fig. 5D). Because this event occurred immediately after the first event that showed the depletion effect, the transported sediment during this event should not come mainly from stream channels but from the hillslope areas near streams, though it had a clockwise loop (Table 1). Thus, the increase of sediment toward the end of the falling limb should be caused by the existence of second sources of sediment nearby the sampling site. Again, the supply-limited nature of sediment transport showed in all events.

3.3. Event sediment yields (SSY_e) and the associated peak discharges (Q_{peak})

In spring, all events can be fitted fairly well by a single curve except the 4/21/2009 event with a clockwise pattern (Fig. 6A). Because stream channels served as the main sediment sources only in this event, the relatively large discrepancy between measured and predicted SSY_e may reflect the different transport processes caused by different sediment sources (stream channels vs. upland sources).

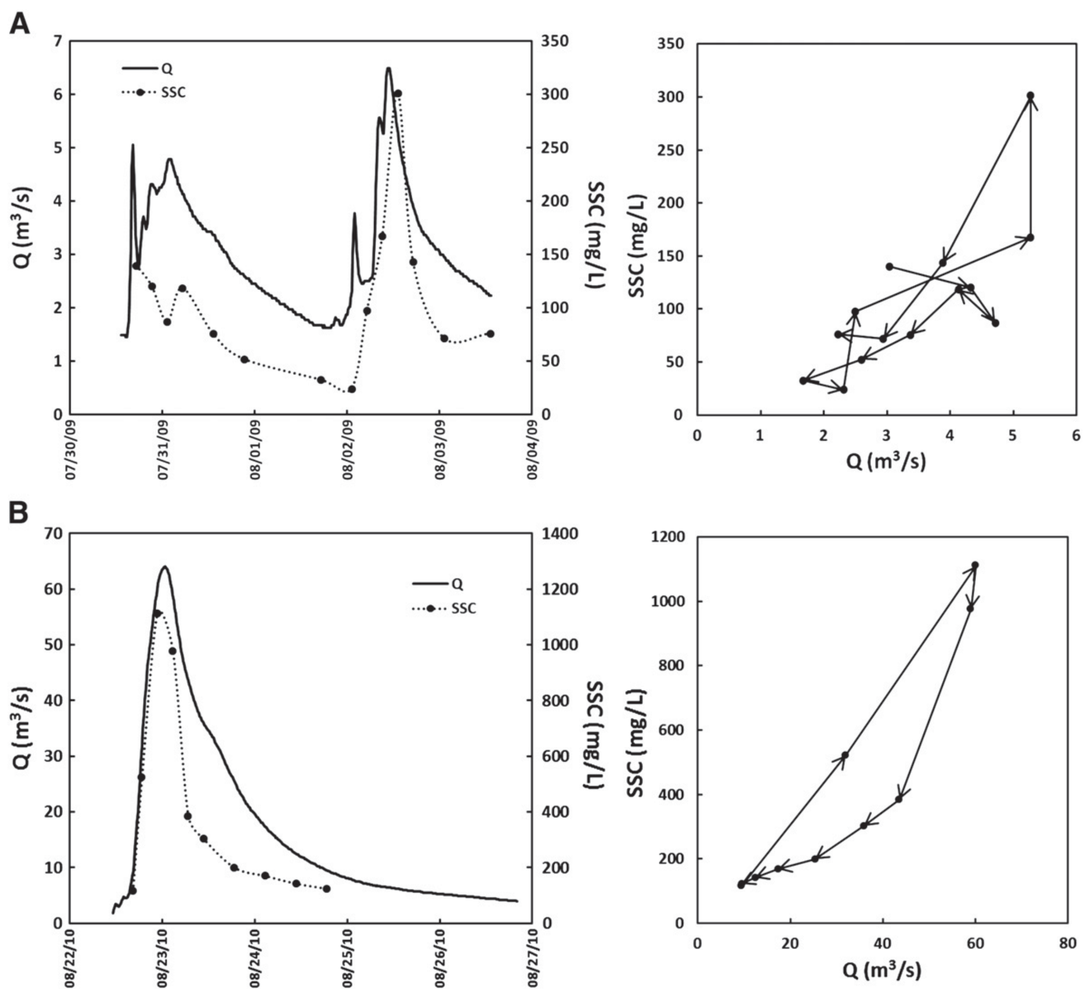

Fig. 4. Different types of hysteresis patterns in summer. (A) A complicated loop in the 7/31/2009 event, (B) a figure-8/C loop in the 8/22/2010 event, (C) a clockwise loop in the 8/11/2008 event, and (D) an anticlockwise loop in the 7/27/2008 event.

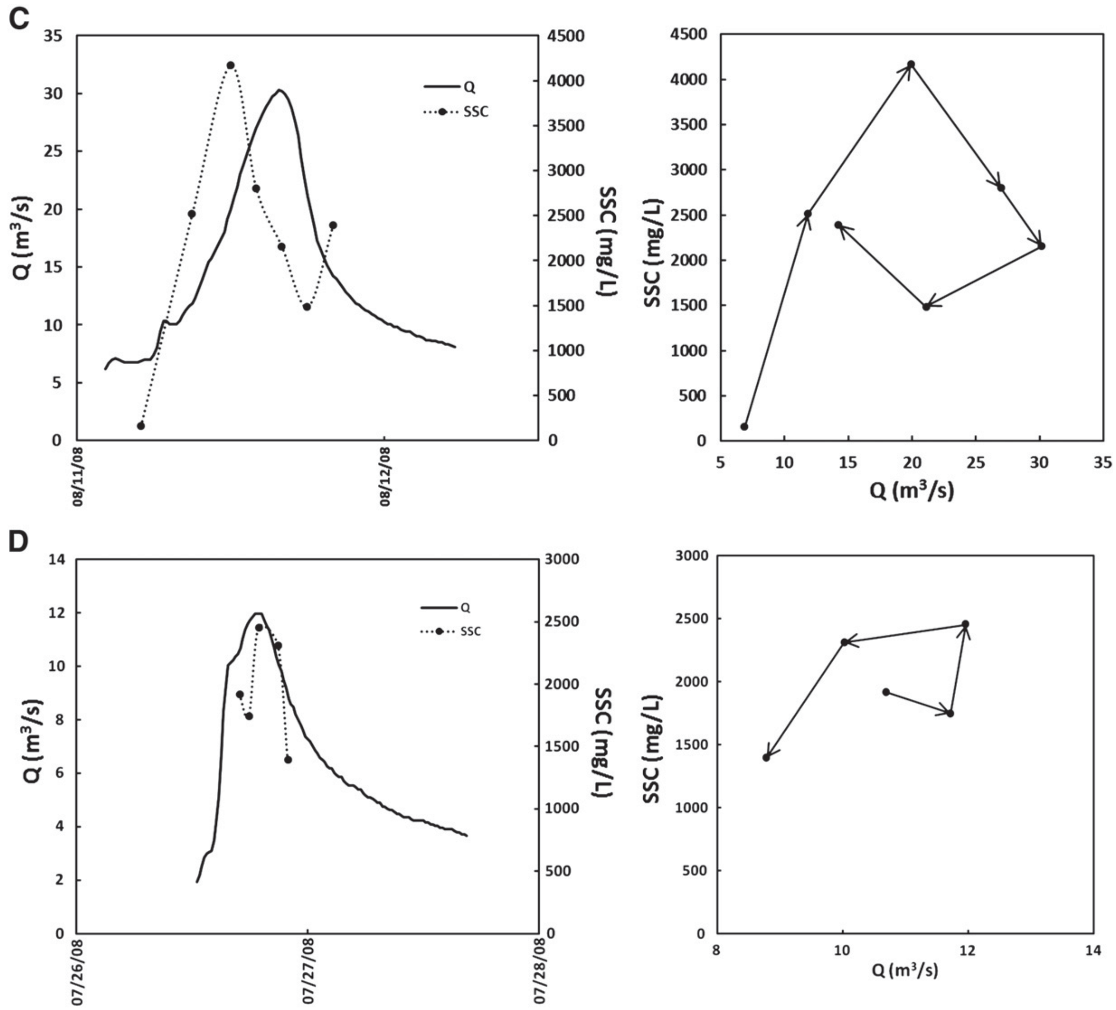

Fig. 4 (*continued*).

However, the statistically significant fitting curve with a high r^2 value signified that SSY_e in the clockwise event statistically belonged to the same population as those of other events in spring, which might reflect that the supply-limited nature commonly existed in all events.

In summer, SSY_e and Q_{peak} pairs were generally plotted around a single curve (Fig. 6B). The largest errors were associated with the clockwise event (8/11/2008) and one anticlockwise event (7/27/2008). The clockwise event, during which sediment was mainly originated from stream channels, tended to produce more sediment for a given Q_{peak} compared with the events of other patterns. This is consistent with the finding in spring. No reasonable transport process was available to account for the large error in the anticlockwise event (7/27/2008). The only plausible explanation is that all sample points (five) were collected during relatively high discharges of the event, resulting in the over-prediction of SSY_e. Nonetheless, the fitting curve not only was statistically significant but also had a relatively high r^2 value implying that the errors created in these two events were not statistically significant. Again, this generally good fitting of the data is related to the supply-limited nature of sediment transport in all events. Thus, the effect of different sediment sources on SSY_e is secondary.

Data in fall and winter were generally characterized very well by the regression curve (Fig. 6C), in particular, those from the three fall events were plotted along the curve regardless of hysteresis loops and where dominant sediment sources were. The winter rainfall event with an anticlockwise loop (12/27/2009) followed the trend of the data representing fall events. Notably, most winter snowmelt events were fitted well by the regression curve except one (3/12/2010). This exception represented the second of the series snowmelt events in winter 2010 with the local sediment supply toward the end, which may explain the relatively high SSY_e. However, the error caused by this event was limited because the regression curve was statistically significant with a high r^2 value, which again coincides with the supply-limited nature of all events.

When data of all seasons were combined, the regression analysis resulted in a statistically significant curve with a high r^2 value (Fig. 6D). This signifies that the data from all seasons essentially belonged to the same population. Therefore, the seasonal differences represented by the three different statistical equations in Fig. 6A–C are statistically insignificant. Although detailed sediment transport processes within each event were diverse, giving rising to different hysteresis loops in each season, the cumulative effect over the event was significantly simplified: event sediment yield throughout all seasons was controlled by a single variable, event peak discharge. Because sediment transport in all events, irrespective of hysteresis patterns, bore the supply-limited feature, the single statistical equation shown in Fig. 6D appears to be the quantitative representation of this nature.

4. Discussion

4.1. Limitations of hysteresis analysis

Hysteresis loops essentially reflect the disparity between water movement and sediment transport during a hydrological event. The hydraulic significance of this disparity is that suspended sediment is not fully controlled by flow hydraulics, which may mechanically be ascribed to two facts: (i) sediment is often transported below capacity (Walling, 1977) and (ii) sediment supply from hillslopes and streams is spatially and temporally variable (Owens et al., 2005). Thus, hysteresis analysis is a useful tool to identify different processes causing *SSC* variation with respect to the associated water discharges. However, hysteresis analysis has suffered a series of limitations.

First, the qualitative nature of judging hysteresis patterns could give rise to inconsistency or uncertainty in identification of the hysteresis patterns. For example, the 12/1/2010 winter event, which was identified as a complicated pattern (Fig. 5B), can alternatively be regarded as the event with a weak loop because all data points may be fitted well by a single regression curve with $r^2 = 0.85$ ($p < 0.01$). Such difference could result in different interpretation of the associated transport processes, though in this case the weak loop pattern also suggested the limited sediment supply from upland sources (otherwise, higher sediment concentrations would have occurred during the falling limb and a separate regression curve may be needed to fit the data in this part of the falling limb separately). Second, when an event has a complicated hysteresis pattern (e.g., 7/31/2009; Fig. 4A), the associated transport processes cannot be simply explained as to whether sediment was from stream channels or upland areas because sediment sources may be changed between the two or both sources made significant contributions to the transported sediment during the event. Third, the classic analysis that links hysteresis patterns to whether Q_{peak} or SSC_{peak} arrives earlier or comparing values of SSC/Q for the two limbs (Williams, 1989) may be confusing (Jansson, 2002). For example, an anticlockwise loop may be caused by an event during which Q_{peak} is earlier than SSC_{peak}, or Q_{peak} is later than SSC_{peak}, or both Q_{peak} and SSC_{peak} arrive simultaneously (Lefrancois et al., 2007; Fang et al., 2008). Fourth, hysteresis patterns are affected by the sizes of the watersheds. For instance, studies have shown that in many small-sized watersheds ($A < 10$ km^2), sediment transport processes are commonly dominated by the clockwise loop (Seeger et al., 2004; Langlois et al., 2005; Lefrancois et al., 2007; Sadeghi et al., 2008b; Smith and Dragovich, 2009). This means even if sediment in such watersheds is sufficiently supplied from hillslope, which would normally lead to an anticlockwise loop, the resultant pattern still tends to be a clockwise loop. The reason is that sediment transport distances between hillslope-outlet and in-channel-outlet are not significantly different. Hence, most sediment originated from hillslope may arrive at the outlet before the peak discharge. In the studied watershed with an area of

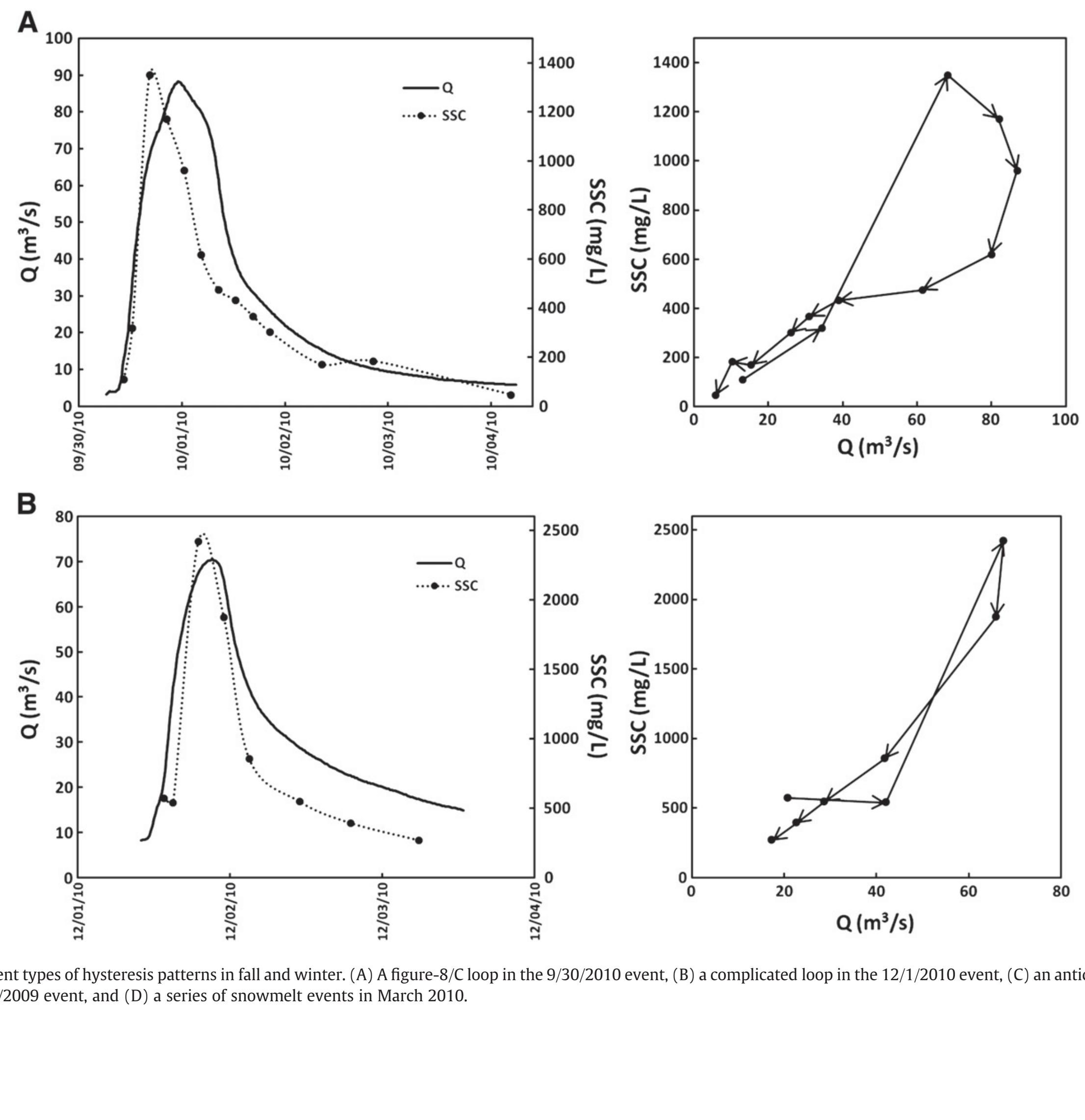

Fig. 5. Different types of hysteresis patterns in fall and winter. (A) A figure-8/C loop in the 9/30/2010 event, (B) a complicated loop in the 12/1/2010 event, (C) an anticlockwise loop in the 12/27/2009 event, and (D) a series of snowmelt events in March 2010.

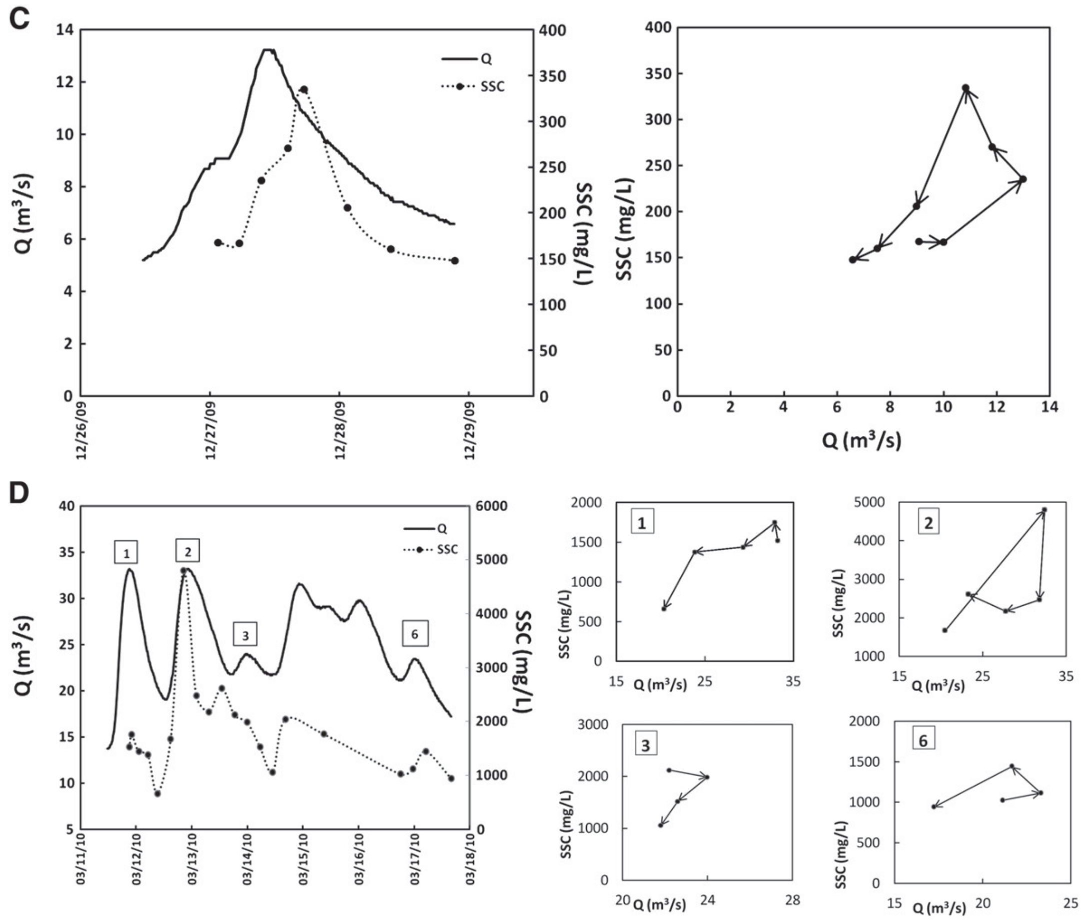

Fig. 5 (*continued*).

311 km², however, a variety of hysteresis loops were found for sediment either from stream channels or upland sources.

These limitations constrain the ability of hysteresis analysis in identifying detailed sediment dynamics of events in the studied watershed. For instance, though the anticlockwise pattern of the 6/5/2010 event (Fig. 3D) indicated that sediment was mainly supplied from upland areas, it could not recognize exactly which parts of the upland were the true sediment sources. Furthermore, hysteresis analysis failed to identify specific processes that caused different hysteresis patterns in the same season. More information based on simultaneous measurements in several subwatersheds is required to overcome the constraints. Nonetheless, the hysteresis analysis successfully revealed the general supply-limited nature of sediment transport in all seasons, which suggests that though sediment dynamics were complicated during individual events, their common supply-limited feature can still be identified by the hysteresis analysis.

4.2. Calculation of SSY_e and the significance of the SSY_e–Q_{peak} relationship

Calculation of event sediment yield (SSY_e) was based on discharge data determined by the established stage–discharge relationships, and the associated sediment rating curve(s) (SRCs) developed using the data collected during each event. The major error in calculating SSY_e came from the poor SRCs in some events because of relatively fewer data points. The impact of such error on SSY_e values was tested using the 5/27/2009 event (Fig. 2A) for three scenarios. In each scenario, we took out a few points from both trends and created a new set of SRCs. Then we calculated SSY_e using these new SRCs. Comparing with the original one calculated using the SRCs in Fig. 2B, the new SSY_e values were all within ±10% of the original one. These results confirmed that in the studied watershed where sediment transport is dominated by the supply-limited nature, *SSC* values between the sparse sampling points were possibly not far away from the trend formed by the values of these points. Therefore, we believe that in the events with relatively fewer data points (e.g., the 6/5/2010 and 7/27/2008 events), errors in the calculated SSY_e values are limited.

The good and statistically significant relationship between SSY_e and Q_{peak} (Fig. 6D) has three important implications. First, though detailed sediment dynamics within each event varied from event to event even in the same season — which was evidenced by diverse hysteresis patterns (Table 1) and variable shapes of the same patterns — their lumped effect over the entire event can be simplified into a quite simple transport process: event sediment yield was dominated by the associated event peak discharge. Second, the simple transport process remains the same for all seasons. This is consistent with the general supply-limited nature of sediment transport in the studied watershed. Thus, the SSY_e–Q_{peak} equation is actually the quantitative representation of the supply-limited nature. Third, given that Q_{peak} may be easily determined using the discharge records from nearby USGS gauging station, the SSY_e–Q_{peak} relationship can serve as a tool for watershed managers to use in practice to predict SSY_e of the studied watershed for any event. Moreover, similar SSY_e–Q_{peak} relationships may be established in other supply-limited watersheds.

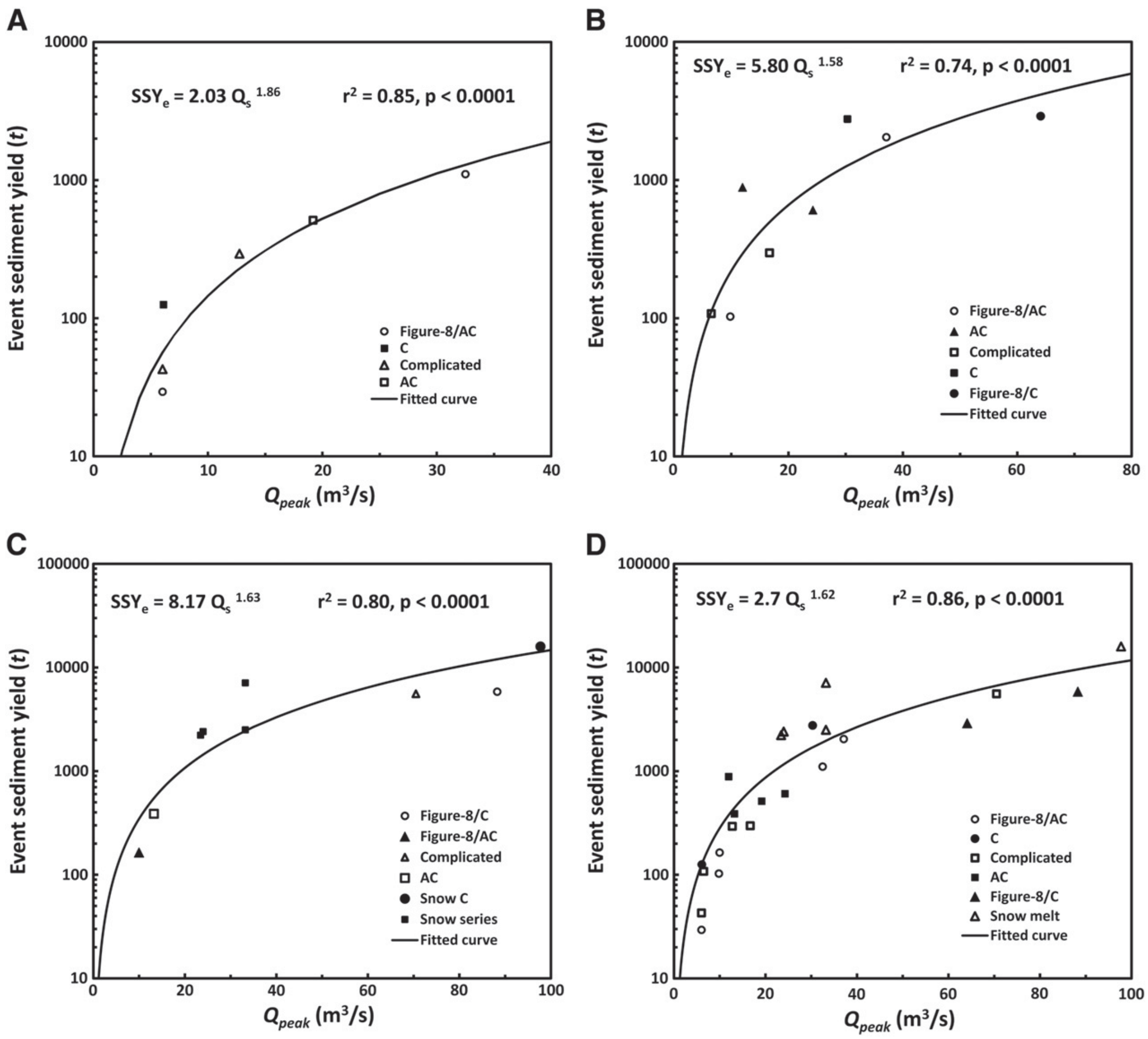

Fig. 6. The SSY_e–Q_{peak} relationship for (A) spring, (B) summer, (C) fall and winter, and (D) the study period.

4.3. Magnitude–frequency analysis of sediment yields

The established SSY_e–Q_{peak} relationship allowed us to further examine the long-term nature of suspended sediment transport in the studied watershed using the magnitude–frequency approach. Similar to the approach used previously (Biedenharn and Thorne, 1994; Hicks, 1994; Mckee and Hossain, 2002), the first step was to determine the threshold discharge Q_t, above which all Q_{peak} will be selected. Using previously developed SRCs for samples collected in 2007 (Gao and Puckett, 2011), we discovered that the total sediment load for events with Q_{peak}<5.66 m^3/s only contributed <10% of the annual sediment yield in 2007. Thus, this value was used as Q_t, based on which we identified 573 above-threshold events from 1990 to 2010. Next, we performed partial flood frequency analysis (McCuen, 2004) and generated the plot showing the relationship between cumulative proportions of 21-year average sediment yields and the associated discharge return periods (Fig. 7).

Over the 21-year period, 66% of sediment load was transported by flows with the recurrence interval (RI)<0.5 year (six months), an additional 22% was transported by flows with the RI falling between 0.5 and 3.1 years, and only 5% was attributed to extreme flows with RI> 15 years. This pattern suggests that annual erosion in the studied watershed is mainly caused by relatively small but more frequent events, which is strikingly distinct from that in badland watersheds where annual erosion is dominated by a few big events (Wainwright, 1996; Fang et al., 2008; Nadal-Romero et al., 2008)

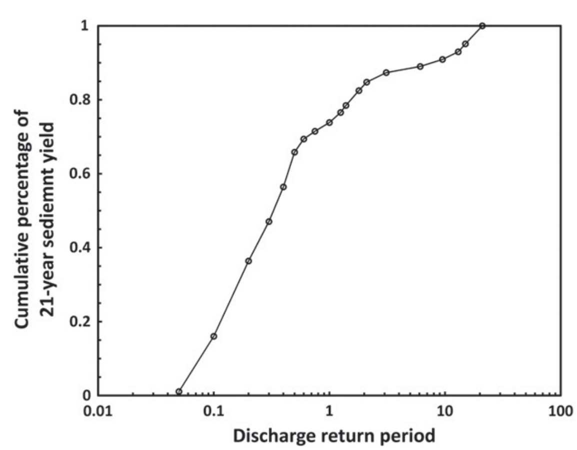

Fig. 7. Plot of cumulative percentage of 21-year sediment yield versus discharge return period.

and from glacier-dominated and French alpine watersheds (Orwin and Smart, 2004; Old et al., 2005; Cockburn and Lamoureux, 2008; Mano et al., 2009).

5. Conclusions

In this study, we examined event sediment dynamics of a 311-km^2 watershed in central New York using data representing 23 rainfall and snowmelt events from 2008 to 2010. Statistical analysis for the four characteristic variables (Q_{mean}, Q_{peak}, SSC_{mean}, and SSC_{peak}) showed that both water discharge (Q) and suspended sediment concentration (SSC) were high in winter and low in spring. Hysteresis analysis identified a variety of hysteresis patterns including clockwise, anticlockwise, figure-8/AC, figure-8/C, complicated, and weak loop patterns appeared during the study period, none of which significantly outnumbered the others in each season and for all seasons. Furthermore, each season showed a different subgroup of these patterns. The variety of hysteresis patterns within and between seasons indicated that sediment dynamics were not only complicated in individual events but also varied among seasons. However, hysteresis analysis revealed that event sediment dynamics were dominated by a common feature: sediment transport over the entire event was supply limited. Therefore, though hysteresis analysis has limited ability to recognize detailed transport processes within an event, it is still capable of identifying that the relatively large watershed is a supply-limited system.

Although events in a season had various hysteresis patterns, their values of Q_{peak} and SSY_e can be described by a single statistical relationship with a trend of overpredicting SSY_e for the clockwise events. In addition, the difference between the Q_{peak}–SSY_e relationships of different seasons is so small that all Q_{peak} and SSY_e pairs may be characterized by a single statistically significant equation. The event sediment yield, SSY_e, represents the comprehensive effect of all detailed transport processes within one event. The fact that a single, statistically significant Q_{peak}–SSY_e relationship exists in the studied watershed suggests that the complicated within-event transport processes can be simplified over the entire period of an event. The simplified process signifies that the event sediment yield is essentially controlled by a single variable, Q_{peak}. This simplified process may indeed reflect the supply-limited nature of sediment transport in the studied watershed. The Q_{peak}–SSY_e equation could be used by watershed managers as a quantitative tool to predict event, seasonal, or annual sediment yields. Combining this equation with the magnitude–frequency analysis further revealed that in the last 21 years, sediment load in the studied watershed was primarily created by relatively small but more frequent discharges with the recurrence interval less than six months.

Acknowledgments

We thank City of Oneida Waste Water Treatment Plant for granting us setting up our monitoring station in its territory. We also thank the three anonymous reviewers for their insightful and constructive comments.

References

Asselman, N.E.M., 1999. Suspended sediment dynamics in a large drainage basin: the River Rhine. Hydrological Processes 13, 1437–1450.
Biedenharn, D.S., Thorne, C.R., 1994. Magnitude–frequency analysis of sediment transport in the lower Missippi River. Regulated Rivers: Research & Management 9, 237–251.
Brasington, J., Richards, K., 2000. Turbidity and suspended sediment dynamics in small catchments in the Nepal Middle Hills. Hydrological Processes 14, 1448–1463.
Cockburn, J.M.H., Lamoureux, S.F., 2008. Hydroclimate controls over seasonal sediment yield in two adjacent High Arctic watersheds. Hydrological Processes 22, 2013–2027.
de Boer, D.H., Campbell, I.A., 1989. Spatial scale dependence of sediment dynamics in a semi-arid badland drainage basin. Catena 16, 277–290.
Domack, E., Ingmire, S., Arnold, K., 2004. Sediment Dynamics of the Oneida Creek Delta, Oneida Lake, New York. Central New York Regional Planning and Development Board, Syracuse, New York.
Fang, H.Y., Cai, Q.G., Chen, H., Li, Q.Y., 2008. Temporal changes in suspended sediment transport in a gullied loess basin: the lower Chabagou Creek on the Loess Plateau in China. Earth Surface Processes and Landforms 33, 1977–1992.
Gao, P., 2008. Understanding watershed suspended sediment transport. Progress in Physical Geography 32, 243–263.
Gao, P., Pasternack, G., 2007. Dynamics of suspended sediment transport at field-scale drain channels of irrigation-dominated watersheds in the Sonoran Desert, southeastern California. Hydrological Processes 21, 2081–2092.
Gao, P., Puckett, J., 2011. A new approach for linking event-based upland sediment sources to downstream suspended sediment transport. Earth Surface Processes and Landforms. doi:10.1002/esp. 2229.
Hicks, D.M., 1994. Land-use effects on magnitude–frequency characteristics of storm sediment yields: some New Zealand examples. Publication No. 224. International Association of Hydrological Science, Canberra, Australia, pp. 395–402.
Hicks, D.M., Gomez, B., 2003. Sediment transport. In: Kondolf, G.M., Piegay, H. (Eds.), Tools in Fluvial Geomorphology. John Wiley & Sons Ltd., Chichester, UK, pp. 425–462.
Jansson, M.B., 2002. Determining sediment source areas in a tropical river basin, Costa Rica. Catena 47, 63–84.
Klein, M., 1984. Anti-clockwise hysteresis in suspended sediment concentration during individual storms. Catena 11, 251–257.
Langlois, J.L., Johnson, D.W., Mehuys, G.R., 2005. Suspended sediment dynamics associated with snowmelt runoff in a small mountain stream of Lake Tahoe (Nevada). Hydrological Processes 19, 3569–3580.
Lawler, D.M., Petts, G.E., Foster, I.D.L., Harper, S., 2006. Turbidity dynamics during spring storm events in an urban headwater river system: the Upper Tame, West Midlands, UK. Science of the Total Environment 360, 109–126.
Lecce, S.A., Pease, P.P., Gares, P.A., Wang, J., 2006. Seasonal controls on sediment delivery in a small coastal plain watershed, North Carolina, USA. Geomorphology 73, 246–260.
Lefrancois, J., Grimaldi, C., Gascuel-Odoux, C., Gilliet, N., 2007. Suspended sediment and discharge relationships to identify bank degradation as a main sediment source on small agricultural catchments. Hydrological Processes 21, 2923–2933.
Lopez-Tarazon, J.A., Batalla, R.J., Vericat, D., Francke, T., 2009. Suspended sediment transport in a highly erodible catchment: the River Isábena (southern Pyrenees). Geomorphology 109, 210–221.
Mano, V., Nemery, J., Belleudy, P., Poirel, A., 2009. Assessment of suspended sediment transport in four alpine watersheds (France): influence of the climatic regime. Hydrological Processes 23, 777–792.
McCuen, R., 2004. Hydrologic Analysis and Design. Pearson Prentice Hall, Upper Saddle River, New Jersey.
Mckee, L.J., Hossain, S., 2002. Magnitude–frequency Analysis of Suspended Sediment Loads in the Subtropical Richmond River basin, Northern New South Wales, Australia. Publication No. 276. International Association of Hydrological Science, Alice Springs, Australia, pp. 289–296.
Nadal-Romero, E., Latron, J., Marti-Bono, C., Regues, D., 2008. Temporal distribution of suspended sediment transport in a humid Mediterranean badland area: the Araguás catchment, central Pyrenees. Geomorphology 97, 601–616.
Oeurng, C., Sauvage, S., Sánchez-Pérez, J., 2010. Dynamics of suspended sediment transport and yield in a large agricultural catchment, southwest France. Earth Surface Processes and Landforms. doi:10.1002/esp. 1971.
Old, G.H., Lawler, D.M., Snorrason, Á., 2005. Discharge and suspended sediment dynamics during two jökulhlaups in the Skaftá River, Iceland. Earth Surface Processes and Landforms 30, 1441–1460.
Orwin, J.F., Smart, C.C., 2004. Short-term spatial and temporal patterns of suspended sediment transfer in proglacial channels, Small River Glacier, Canada. Hydrological Processes 18, 1521–1542.
Owens, P.N., Batalla, R.J., Collins, A.J., Gomez, B., Hicks, D.M., Horowitz, A.J., Kondolf, G.M., Marden, M., Page, M.J., Peacock, D.H., Petticrew, E.L., Salomons, W., Trustrum, N.A., 2005. Fine-grained sediment in river systems: environmental significance and management issues. River Research and Applications 21, 693–717.
Park, J., 1992. Suspended sediment transport in a mountainous catchment. The Science Reports of the Institute of Geoscience. University of Tsukuba, South Korea, pp. 137–197.
Picouet, C., Hingray, B., Olivry, J.C., 2001. Empirical and conceptual modelling of the suspended sediment dynamics in a large tropical African river: the Upper Niger River basin. Journal of Hydrology 250, 19–39.
Richards, G., Moore, R.D., 2003. Suspended sediment dynamics in a steep, glacier-fed mountain stream, Place Creek, Canada. Hydrological Processes 17, 1733–1753.
Rieger, W.A., Olive, J., Gippel, C.J., 1988. Channel sediment behaviour as a basis for modelling delivery processes. Publication No. 174. International Association of Hydrological Science, Porto Aiegre, Brazil, pp. 541–548.
Rovira, A., Batalla, R.J., 2006. Temporal distribution of suspended sediment transport in a Mediterranean basin: the lower Tordera (NE Spain). Geomorphology 79, 58–71.
Sadeghi, S.H.R., Mizuyama, T., Miyata, S., Gomi, T., Kosugi, K., Fukushima, T., Mizugaki, S., Onda, Y., 2008a. Determinant factors of sediment graphs and rating loops in a reforested watershed. Journal of Hydrology 356, 271–282.
Sadeghi, S.H.R., Mizuyama, T., Miyata, S., Gomi, T., Kosugi, K., Fukushima, T., Mizugaki, S., Onda, Y., 2008b. Development, evaluation and interpretation of sediment rating curves for a Japanese small mountainous reforested watershed. Geoderma 144, 198–211.

Schmidt, K., Morche, D., 2006. Sediment output and effective discharge in two small high mountain catchments in the Bavarian Alps, Germany. Geomorphology 80, 131–145.

Seeger, M., Errea, M.-P., Beguería, S., Arnáez, J., Martí, C., García-Ruiz, J.M., 2004. Catchment soil moisture and rainfall characteristics as determinant factors for discharge/suspended sediment hysteretic loops in a small headwater catchment in the Spanish Pyrenees. Journal of Hydrology 288, 299–311.

Singh, V.P., 1995. Watershed modeling. In: Singh, V.P. (Ed.), Computer Models of Watershed Hydrology. Water Resources Publications, Littleton, CO, pp. 1–22.

Smith, H.G., Dragovich, D., 2009. Interpreting sediment delivery processes using suspended sediment-discharge hysteresis patterns from nested upland catchments, south-eastern Australia. Hydrological Processes 23, 2415–2426.

Wainwright, J., 1996. Infiltration, runoff and erosion characteristics of agricultural land in extreme storm events, SE France. Catena 26, 27–47.

Walling, D.E., 1977. Limitations of the rating curve technique for estimating suspended sediment loads, with particular reference to British rivers. Publication No. 122. International Association of Hydrological Science, Paris, France, pp. 34–47.

Walling, D.E., Webb, B.W., 1982. Sediment availability and prediction of storm-period sediment yield. Publication No. 137. International Association of Hydrological Science, Exeter, UK, pp. 327–337.

Williams, G.P., 1989. Sediment concentration versus water discharge during single hydrologic events in rivers. Journal of Hydrology 111, 89–106.

Wotling, G., Bouvier, C., 2002. Impact of urbanization on suspended sediment and organic matter fluxes from small catchments in Tahiti. Hydrological Processes 16, 1745–1756.

Yildiz, O., 2004. An investigation of the effects of drainage density on hydrologic response. Turkish Journal of Engineering & Environmental Sciences 28, 85–94.